# Multiscale modeling in Nanotechnology

A. Maiti*

*Accelrys Inc., 9685 Scranton Road, San Diego, CA 92121

## ABSTRACT

Technologically important nanomaterials come in all shapes and sizes. They can range from small molecules to complex composites and mixtures. Depending upon the spatial dimensions of the system and properties under investigation, computer modeling of such materials can range from first-principles Quantum Mechanics, to Forcefield-based Molecular Mechanics, to mesoscale simulation methods. In this contribution we illustrate the use of all three modeling techniques through a number of recent applications: (1) carbon nanotubes (CNTs) as nano electromechanical sensor (NEMS) devices; (2) mesoscale modeling of polymer-nanotube composites; and (3) mesoscale diffusion of drug molecules across cell membranes.

***Keywords***: nanotubes, nanocomposites, mesoscale modeling, membranes, diffusion.

## 1 INTRODUCTION

As with any new technology, Nanotechnology has many challenges to overcome, typically associated with control and precision at the nanoscale. Some of the challenges include: device integration (interconnect failure, addressability issues), growth and synthesis (difficulty in size-dispersion control, requirement of novel assembly techniques, presence of structural defects), contact resistance (necessity of atomic-level structural precision at junctions), functionalization (challenges with chemical inertness) and doping (non-uniformity of dopant levels). Computer modeling is a great approach to surmounting some of the above obstacles because it often provides deeper insight into the system properties as a function of size/shape, structural defects, added functional groups, and system surroundings. However, the simulation method and the resolution details depend upon the system size and the properties to be investigated. Thus, to study electronic structure one has to take recourse to a Quantum mechanical method, either First-Principles or semi-empirical. To study electronic transport, one has to use a code based on the non-equilibrium Green's function (NEGF) formalism. To investigate macro-molecular structures like DNA, proteins or large nanotubes, one would employ classical molecular mechanics based on force fields, while investigations of phenomena at larger length and time-scales would require the use of mesoscale and possibly finite-elements methods. This work illustrates the use of several of the above simulation techniques in three different application areas: (1) CNTs as NEMS devices; (2) polymer-nanotube composites; and (3) drug diffusion across cell membranes.

## 2 CNT-BASED ELECTROMECHANICAL SENSORS

Interest in the application of carbon nanotubes as electromechanical sensors got a significant boost from the pioneering experiment of Tombler *et al.* [1], in which the middle part of the segment of a metallic CNT suspended over a trench was pushed with an Atomic Force Microscope (AFM) tip. Beyond a deformation angle of ~ 13° the electrical conductance of the tube dropped by more than two orders of magnitude. The effect was found to be completely reversible, *i.e.*, through repeated cycles of AFM-deformation and tip removal, the electrical conductance displayed a cyclical variation with constant amplitude. An interesting explanation was put forward by O(N) tight-binding calculations [2], which show that beyond a critical deformation several C-atoms close to the AFM tip become $sp^3$-coordinated. This leads to the tying up of $\pi$-electrons into localized $\sigma$-states, which would explain the large drop in electrical conductance.

Considering the significance of the above result, it was important to carry out an independent investigation using first-principles QM. Unfortunately, the smallest models required to simulate the AFM-deformation of a CNT typically involve a few thousand atoms, which makes first-principles QM simulations unfeasible. This necessitated a combination of first-principles DFT and classical molecular mechanics. Bond reconstruction, if any, is likely to occur only in the highly deformed, non-straight part of the tube close to the AFM-tip. For such atoms (~ 100-150 atoms including AFM-tip atoms) a DFT-based QM description was used, while the long and essentially straight part away from the AFM tip was described accurately using the Universal Forcefield (UFF) [3], which had previously been used in CNT simulations [4].

Because of known differences in the electronic response of zigzag and armchair tubes to mechanical deformation, the simulations were performed on a (12, 0) zigzag and a (6, 6) armchair tube, each consisting of 2400 atoms. The AFM tip was modeled by a 6-layer deep 15-atom Li-needle normal to the (100) direction, terminating in an atomically sharp tip. To simulate AFM-tip-deformation, the Li-needle was initially aimed at the center of a hexagon on the bottom-side of the middle part of the tube. The Li-

needle tip was then displaced by an amount $\delta$ toward the tube along the needle-axis, resulting in a deformation angle $\theta = tan^{-1}(2\delta / l)$, $l$ being the unstretched length of the tube. At each end of the tube, a contact region defined by a unit cell plus one atomic ring (a total of 36 and 60 atoms for the armchair and the zigzag tube respectively) was then fixed and the whole tube relaxed with the UFF, while constraining the needle atoms as well. The contact region atoms were fixed in order to simulate an ideal undeformed semi-infinite carbon nanotube lead, and to ensure that all possible contact modes are coupled to the deformed part of the tube. Following the UFF relaxation, a cluster of 132 C-atoms for the (6, 6) tube, and a cluster of 144 C-atoms for the (12, 0) tube were cut out from the middle of the tubes. These clusters, referred to below as the *QM clusters* (plus the 15 Li-tip atoms) were further relaxed with Accelrys' DFT-code DMol$^3$ [5], with the end atoms of the cluster plus the Li-tip atoms fixed at their respective classical positions.

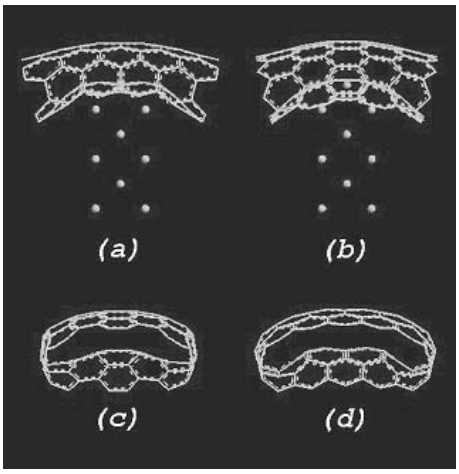


Figure 1. DMol$^3$-relaxed Li-tip-deformed QM clusters for: (a) the (6, 6) armchair (132 C-atoms); and (b) the (12, 0) zigzag (144 C-atoms), in side views. The deformation angle is 25º for both tubes. Figs. (c) and (d) are respective views along the tube length, with the Li-tip hidden for clarity.

Fig. 1 displays the tip-deformed QM-cluster for (6, 6) and (12, 0) tubes at the highest deformation angle of 25º considered in these simulations. Even under such large deformations, there is no indication of sp$^3$ bonding, and the structure was very similar to what was observed for a (5, 5) tube in a previous work. The absence of sp$^3$ coordination is inferred based on an analysis of nearest-neighbor distances of the atoms with the highest displacements, *i.e.*, the ones closest to the Li-tip. *Although for each of these atoms the three nearest neighbor C-C bonds are stretched to between 1.45-1.75 Å, the distance of the fourth neighbor, required to induce sp$^3$ coordination is greater than 2.2 Å for all tubes in our simulations.*

Following the structural relaxation of the CNTs, the transmission and conductance were computed using the recursive Green's function formalism [6]. A nearest-neighbor sp$^3$ tight-binding Hamiltonian in a non-orthogonal basis was chosen, and ideal semi-infinite contacts assumed at both ends. These simulations indicate that the conductance remains essentially constant for the (6, 6) armchair tube up to deformation as large as 25°. However, for the (12, 0) zigzag tube the conductance drops significantly, by two orders of magnitude at 20º, and 4 orders of magnitude at $\theta$=25° [7]. Since sp$^3$ coordination could be ruled out, what could be the cause for such a large conductance drop in the experiment of ref. [1]? Also, why did the armchair tube display no significant drop in conductance even up to large angles of deformation?

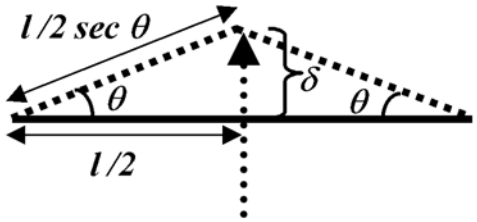


Figure 2. Schematic diagram representing deformation with an AFM tip. The tip-deformed tube undergoes a tensile strain. The deformation angle $\theta$ is related to the tip displacement ($\delta$) and non-deformed tube-length ($l$) by $\theta = tan^{-1}(2\delta / l)$.

A simple explanation emerges if one zooms out from the middle of the tube and looks at the profile of the whole tube under AFM-deformation. One immediately discovers an overall stretching of the tube under AFM-deformation, as indicated schematically in Fig. 2. The effect of tensile stretch on CNT conductance has been theoretically studied in great detail [8]. An important result from such studies is that the *rate of change* of bandgap as a function of strain depends on the CNT chiral angle $\theta$, more precisely as proportional to $cos(3\theta)$. Thus, stretched armchair tubes ($\theta$ = 30º) do not open any bandgap, and always remain metallic. On the other hand, a metallic ($3n$, 0) zigzag tube ($\theta$ = 0) can open a bandgap of ~100 meV when stretched by only 1%. This bandgap increases linearly with strain, thus transforming the CNT into a semiconductor at a strain of only a few percent. In general, all metallic tubes with $n_1 - n_2 = 3n$ will undergo the above metal-to-semiconductor transition, the effect being the most pronounced in metallic zigzag tubes. An experiment as in ref. [1] is thus expected to show a decrease in conductance upon AFM-deformation for all metallic CNTs except the armchair tubes. Researchers are also beginning to explore the electromechanical response of a squashed CNT, where sp$^3$ coordination is a possibility.

In addition to the above results for metallic CNTs, theory also predicts that for semiconducting tubes ($n_1 - n_2 \neq 3n$), the bandgap can either increase (for $n_1 - n_2 = 3n$ -2) or decrease (for $n_1 - n_2 = 3n$ -1) with strain. These results have recently prompted more detailed experiments on a set of metallic and semiconducting CNTs deformed with an AFM-tip [9], as well as on CNTs under experimental tensile stretch [10]. Commercial applications from such work could lead to novel pressure sensors, transducers, amplifiers, and logic devices [11].

## 3 CNT-POLYMER NANOCOMPOSITES

CNTs are found to possess remarkable mechanical and electrical properties. As discussed in the previous section, the CNTs can be metallic or semiconducting depending upon their chirality. The metallic CNTs are much more conducting than copper, and can carry very high density of electrical currents. Mechanically, the CNTs are stronger than steel yet being much lighter. One would like to utilize such unique properties of CNTs by enhancing mechanical and electrical properties of polymers through dispersing CNTs into a polymeric matrix. Such composites have potential applications not only as structural materials [12] but also for functional applications that make use of their conductivity, electromagnetic interference shielding [13] and optoelectronic properties [14].

The overall properties of CNT-polymer composite material depend on how uniformly the CNTs are dispersed within the polymeric matrix, how effective the interfacial bonding between the two systems is, and the way in which the above properties depend on the nanotube diameter, chirality, and functionalization of the CNT surface with organic functional groups.

There have been a few atomistic studies of the interaction of specific polymers with small segments of isolated CNTs [15]. However, extension of such studies to composites with several CNTs, each a few nanometers long, is extremely difficult because of: (1) a huge number of atoms involved; (2) long time-scales associated with typical dispersion processes. To surmount these challenges, we have adopted a mesoscale approach, in which groups of atoms are lumped into single "beads".

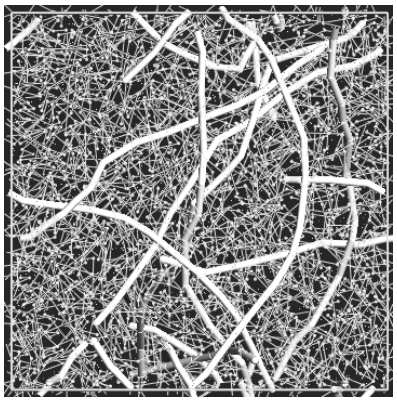

Fig. 3. Snapshot from a DPD simulation of CNTs well dispersed in an amorphous polymeric matrix.

The mesoscale simulations were performed using the code DPD (Dissipative Particle Dynamics) [16]. DPD simulates soft spherical beads interacting through a simple pair-wise potential, and thermally equilibrated through a Langevin thermostat. The total force on each DPD particle (bead) is expressed as a sum of three pair-wise additive terms [17]: (1) a conservative force, which is taken to be a soft repulsion; (2) a dissipative force, proportional to the relative velocity of the beads; and (3) a random force, necessary to maintain the system temperature. For polymeric systems, one has to include an additional interaction due to "springs" connecting the monomeric "beads". While the dissipative and random forces act in unison as a thermostat for the simulation, it is the conservative soft repulsive force that embodies the essential chemistry of the system. Ideally, one would like to derive the conservative force from detailed atomistic interactions. In 1997, Groot and Warren [17] made an important contribution on this front by establishing a relation between a simple functional form of the conservative repulsion in DPD and the Flory-Huggins $\chi$-parameter theory.

The scaling of the repulsive interaction as a function of the bead-size, and its relation to surface tension in strongly segregated systems were recently analyzed by Maiti and McGrother [18]. This work was used to derive the interaction parameters for a CNT-polymer nanocomposite system. In addition, extra "spring" and "angle"-dependent terms were introduced in order to reproduce the Young's modulus and bending rigidity of the CNTs, which were computed from atomistic simulations. Details will be described elsewhere. Fig. 3 is a snapshot from a DPD simulation on a nanocomposite containing a volume fraction of 5% CNT and 95% polymer. The solubility parameters of the CNT and the polymer were close enough in this simulation, which resulted in a uniform dispersion of the CNT within the polymer. Such mixing is necessary for good mechanical properties of the composite. On the other hand, if the solubility parameter of the CNT differs from that of the polymer by a critical amount, it results in bundles of CNTs segregating out of the polymer, as illustrated in Fig. 4. Ongoing simulations are exploring the possibility of aligning the CNTs within the polymer matrix [[19], [20]] through the application of an external shear. Investigations of the effect of attaching organic functional groups to the CNTs are also underway.

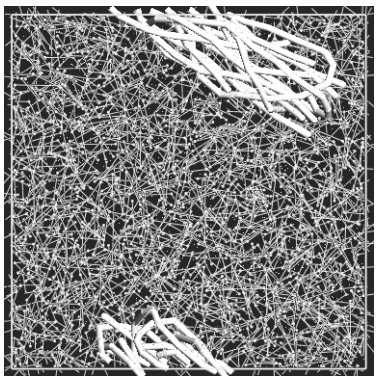

Fig. 4. Mesoscale CNT bundles segregated from a polymeric matrix.

Finally, we are exploring possibilities of importing such mesoscale data into a Finite-elements code [21] that would yield important mechanical and electrical properties of the system as a function of the mesoscale morphology.

## 4. DRUG DIFFUSION THROUGH CELL-MEMBRANE

DPD and other mesoscale modeling codes have so far been primarily used in the study of simple organic liquids, oil/water/surfactant systems, polymer blends, polymeric micelles, and so on. However, since most biological systems are organic in nature, such codes can be extended to the study of biological processes as well. Here we illustrate a novel application of DPD by simulating the diffusion of an Aspirin molecule across a cell membrane.

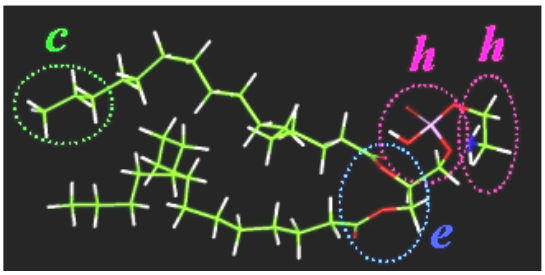


Fig. 5. DPD Bead representation of phospholipids PE.

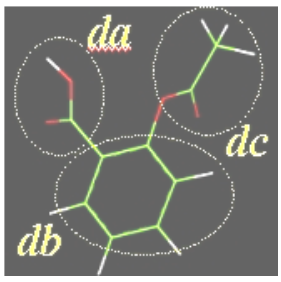


Fig. 6. DPD Bead representation of Aspirin.

A cell membrane typically consists of a lipid bilayer (phospholipids, glycolipids, cholesterol), transmembrane proteins (structural, transport, and channel proteins), and receptors (sugar, protein, etc.). To start with, we chose just a bilayer of the phospholipid phosphatidylethanolamine (PE) [22], whose atomic structure and corresponding mesoscopic beads are shown in Fig. 5. The atomic structure and meso-representation of the drug Aspirin is shown in Fig. 6. The hydrocarbon *c*-beads are hydrophobic, while the "head group" *h*-beads are hydrophilic. The connectivity of the lipid is described as $c_5e_1[h_2]c_5$ (where [] denotes a branching out), while that of the drug is simply $da_1db_1dc_1$. We have attempted a full atomic-scale simulation of the diffusion of Aspirin through the PE-bilayer. However, nothing significant happens in terms of diffusion within a few nanoseconds of simulation times that we are limited to. On the other hand, in a mesoscale simulation (see Fig. 7 for a snapshot), the soft repulsion allows a basic time-step of ~ 100 ps. This fact, coupled with an order of magnitude reduction in the number of beads (as compared to the number of atoms), and much simpler functional form of the DPD interaction (compared to the complex analytical form of typical force fields), effectively leads to *milliseconds* of simulation time within days on a single processor of a typical workstation. Preliminary results indicate trans-membrane diffusion of Aspirin within a few microseconds.

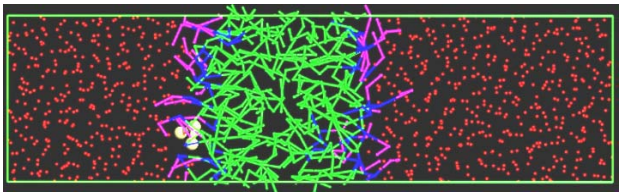

Fig. 7. Mesoscale representation of a three-bead Aspirin diffusing through a PE bilayer. The drug molecule is shown in ball and stick (yellow) representation for clarity. Red beads represent water.

To our knowledge, this is the first mesoscale simulation of drug diffusion across membranes. Current investigations include: (1) studying relative diffusion rates of different drugs; (2) effect of cholesterol content in the membrane; (3) diffusion of hydrophobic drugs encased in a micelle, where processes like endocytosis is a possibility.

**ACKNOWLEDGEMENTS:** The author would like to acknowledge collaborations with M. P. Anantram and Alexei Svizhenko (NASA), and Simon McGrother, James Wescott, and Paul Kung (Accelrys).

## REFERENCES

[1] T. W. Tombler *et al.*, Nature 405, 769, 2000.
[2] L. Liu *et al.*, Phys. Rev. Lett. 84, 4950, 2000.
[3] A. K. Rappe *et al.*, J. Am. Chem. Soc. 114, 10024, 1992.
[4] N. Yao & V. Lordi, J. Appl. Phys. 84, 1939, 1998.
[5] http://www.accelrys.com/mstudio/dmol3.html.
[6] A. Svizhenko *et al.*, J. Appl. Phys. 91, 2343, 2002.
[7] A. Maiti, A. Svizhenko, and M. P. Anantram, Phys. Rev. Lett. 88, 126805, 2002.
[8] L. Yang and J. Han, Phys. Rev. Lett. 85, 154, 2000.
[9] E. D. Minot *et al.*, Phys. Rev. Lett. 90, 156401, 2003.
[10] J. Cao *et al.*, Phys. Rev. Lett. 90, 157601, 2003.
[11] A. Maiti, Nature Materials (London) 2, 440, 2003.
[12] D. Qian *et al.*, Appl. Phys. Lett. 76, 2868, 2000.
[13] J. Sandler *et al.*, Polymer 40, 5967, 1999.
[14] H. Ago *et al.*, Adv. Mater. 11, 1281, 1999.
[15] S. B. Sinnott et al., Carbon 36, 1, 1998; Y. Hu *et al.*, Composites Science & Technology 63, 1663, 2003; M. in het Panhuis *et al.*, J. Phys. Chem. B 109, 478, 2003.
[16] http://www.accelrys.com/mstudio/ms_modeling/dpd.html
[17] R. D. Groot and P. B. Warren, J. Chem. Phys. 107, 4423, 1997.
[18] A. Maiti and S. McGrother, J. Chem. Phys. (in press).
[19] R. Haggenmueller *et al.*, Chem. Phys. Lett. 330, 219, 2000.
[20] C. Bower *et al.*, Appl. Phys. Lett. 74, 3317, 1999.
[21] A.A. Gusev Macromolecules 34, 3081, 2001.
[22] R. D. Groot and K. L. Rabone, Biophysical Journal 81, 725, 2001.